Preparation and characterization of doped titanium dioxide thin films

H. YANG[*], Q. TAO

Department of Inorganic Materials, School of Resources Processing and Bioengineering, Central South University, Changsha 410083, P. R. China

Sn, Ce doped and Sn/Ce co-doped TiO_2 thin films (ST, CT and SCT, respectively) deposited on indium-doped tin oxide (ITO) glass were prepared using sol-gel dip coating technique and were characterized by X-ray diffraction (XRD), X-ray photoelectron spectroscopy (XPS), atomic force microscopy (AFM) and ultraviolet-visible (UV-vis) absorption. The XRD results of the powder samples only showed peaks corresponding to anatase TiO_2 but no crystalline phases of compounds formed by doping ions. XPS studies demonstrated that Sn exists in the form of Sn^{4+}, while Ce exists in the two forms of Ce^{3+} and Ce^{4+}. The UV-vis spectra revealed that the absorption edges of the doped TiO_2 films exhibits red shift compared with the pure TiO_2 film and the red shifting is the most evident for CT, indicating that doping of Sn and Ce causes the narrowing of the band gap.

1. Introduction

Titanium dioxide (TiO_2), as a typical n-type semiconductor, is a widely used material for many applications such as optical coating [1,2], gas sensor [3,4], photocatalysis [5,6] and solar cell [7-9] due to its favorable physical, chemical, no toxicity, opto-electrical properties, good photocatalytic activity as well as long-term stability. As TiO_2 thin films not only have these above advantages but also are more recuperative than TiO_2 powders [10], they are attracting increasing attentions. TiO_2 has three different crystalline phases: anatase, rutile and brookite. The brookite is very unstable and has no applications. Anatase is a less stable phase and it transforms to rutile at temperature higher than 600°C. The band gap energy is 3.2 eV for anatase and 3.0 eV for rutile, only allowing ultraviolet (UV) absorption which only occupies no more than 5% solar energy. So the wide band gap prevented the highly efficient use of TiO_2 nanomaterials.

Thus, many efforts have been done to the modifications of TiO_2 films [11-22] and the most common modification method is doping TiO_2 with other elements. In recent years, impurity doping has been widely performed by a variety of methods in order to improve TiO_2 thin film's properties [13-16,19,21,22]. Mahanty reported that Sn hinders anatase growth and facilitates anatase to rutile phase transformation and the band gap of rutile $Sn_xTi_{1-x}O_2$ solid solutions increases with increasing x [13]. Du found that all Mo ions doped films show improved heating induced hydrophilicity and the 0.75 wt% Mo ions doped film shows superhydrophilicity after being heated at 400°C for 1 h.[15] Umebayashi and his co-workers synthesized titanium dioxide (TiO_2) doped with sulfur by oxidation annealing of titanium disulfide (TiS_2) and found

that S doping caused the absorption edge of TiO_2 to be shifted into the lower-energy region and contributed to the band gap narrowing [19]. In addition, Lindgren showed that the new band gap states created by the doping nitrogen indeed improve the photoresponse for white light at the expense of some losses of UV response [21].

In this study, Sn, Ce doped and Sn/Ce co-doped TiO_2 thin films (abbreviated ST, CT and SCT, respectively) were prepared. As both Sn and Ce exist in the form of +4 valence for their relatively stable oxide and the doping ions may have some unusual effects on the TiO_2 (Ti^{+4}), we may obtain TiO_2 thin films with special and favorable properties. Preparation method here used is sol-gel dip coating technology. This paper aims to investigate the surface morphology and structure and optical properties of the doped TiO_2 thin films.

2. Experimental

The reactants are all AR grade and used without further purification. Colloidal titanium was prepared as follows: a sol was prepared by mixing 34ml tetrabutylorthotitanate ($Ti(OC_4H_9)_4$), 100ml ethanol (C_2H_5OH) and 9.6ml diethanolamine ($C_4H_{11}NO_2$). After the sol being magnetic stirred for 10 min, 1.76g $SnCl_4.5H_2O$ dissolved in 10 ml ethanol were added to the sol drop by drop with keeping vigorous stirring. Later, a mixture of 1.8 ml distilled water with 30 ml ethanol was added dropwise. Water was used for hydrolysis and polycondensation of $Ti(OC_4H_9)_4$ and diethanolamine was acted as chelating agent. The TiO_2 sol was vigorously stirred for 2h and then a transparent precursor sol was obtained. The Ce-doped sol was made in the same way

only with $CeCl_3.7H_2O$ substituting $SnCl_4.5H_2O$. The SCT TiO_2 sol was made by mixing the above two fresh sols with the same volume together and stirring for 2h. In each case, the metal ion: titanium (1:20) in molar ratio. Usually the resulting TiO_2 sol was aged for 24h at ambient temperature for coating.

TiO_2 thin films deposited on the ITO glass were prepared using the above TiO_2 sol solutions by the dip-coating method. The glass was ultrasonically cleaned in dense H_2SO_4 solution for 30min, then in ethanol for 15min and last in deionized water for 15min. The film thickness was adjusted by dip-coating cycles. Here six layers were deposited on the glass at a withdrawing speed of 4 cm/min using the TL 0.01 dip coater made by MTI Corporation. After a layer was deposited, the glass was treated at 100°C for 5min, and then coating another layer. The glass was thermal treated at 500°C for 2h after six layers were finished.

The structures of doped TiO_2 powder which have the same chemical composition as the TiO_2 films, were investigated by X-ray diffraction (XRD) (Rigaku, D/max-γA, CuKα radiation).The surface morphology was examined by a NT-MDT atomic force microscopy (AFM) with silicon probe tapping contact mode. UV-vis analysis of TiO_2 films were performed on a UV-2450 spectrophotometer. The surface composition and chemical states of the films were analyzed by X-ray photoelectron spectroscopy (XPS) using Mg Kα radiation on a ESCALAB MK II surface analyzer.

3. Results and discussion

Fig. 1 only shows XRD patterns of powder samples (pure, Sn , Ce doped and Sn/Ce co-doped TiO_2 sol after dried at 100 °C for several hours then thermal treated at 500°C for 2h) as the film is too thin to be investigated by XRD technology.

XRD patterns of the three doped TiO_2 are fairly similar to that of the pure TiO_2 and all these diffraction peaks can be indexed to anatase phase of TiO_2 (JCPDS 21-1272). However, no phase of compounds formed by doping ions is found. Some believed that the dopant ions disperse uniformly into the TiO_2 solution and incorporate into the lattice of TiO_2 when the radius of dopant ion is smaller or close to that of Ti.[23-24] As radius of Sn and Ce ions is larger than that of Ti ion, it may be impossible for the doped ions incorporate into the lattice of TiO_2. It is more probable that doping amount is too small to be detected by XRD technology. For pure TiO_2, the intensity of the peak at about 25° corresponding to the plane (101) is obviously higher than the other three doped ones. The average crystal sizes (D) were calculated based on the Scherrer's formula and the results demonstrate that pure TiO_2 has larger crystal size than the doped ones, which indicate that the doping can inhibit growth of the particles.
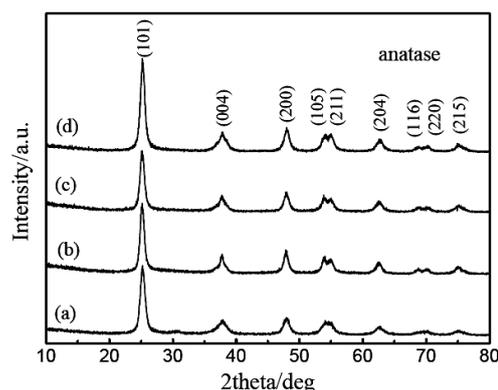
Fig. 1. XRD patterns of (a) Sn, (b) Ce doped, (c) Sn/Ce co-doped and (d) pure TiO_2 powder.

X-ray photoelectron spectroscopy (XPS) is a sensitive and reliable method for investigating the surface composition and chemical state for the films. The full survey spectra of the pure, ST and CT are shown in Fig. 2A, which indicates that the films contain Ti, O, Sn, Ce and trace amounts of C which was used for exterior reference. Ti 2p peaks of doped films didn't exhibit obvious shift compared with that of pure film and the Ti $2p_{3/2}$ and Ti $2p_{1/2}$ peaks located at about 458.2eV and 463.8 eV suggested that Ti exists mainly in the form of Ti^{4+} for all the films.

(a)

(b)
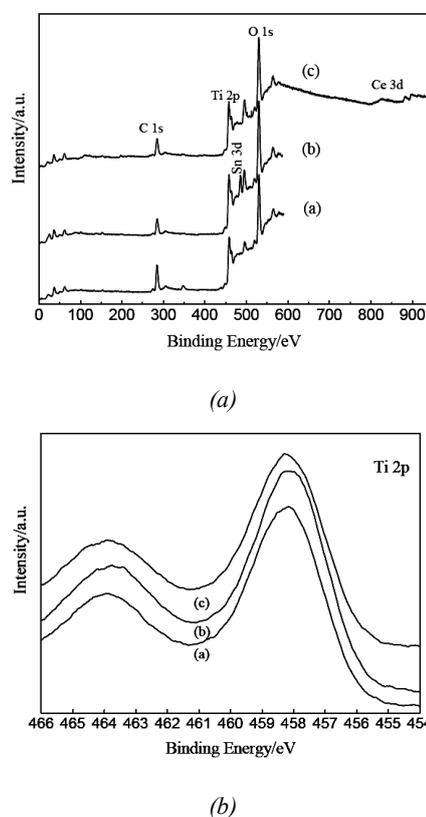
Fig. 2. Full survey spectra (A) and XPS of Ti 2p (B) for (a) pure film (b) ST and (c) CT.

Generally binding energy (BE) of Sn $3d_{5/2}$ for SnO is very close to that for SnO_2 (less than 0.7 eV separations) and the distinction between them is ambiguous. Here Sn $3d_{5/2}$ peak located at about 486 eV , the presence of metallic Sn can be ruled out as Sn $3d_{5/2}$ 484.6 eV for the metallic tin. It corresponds to Sn^{4+} according to literature.[25] From the full survey spectra in Fig. 2B(c), we can see the peaks corresponding to Ce 3d electron region are weak due to the relatively small amount of Ce on the film.

(a)

(b)
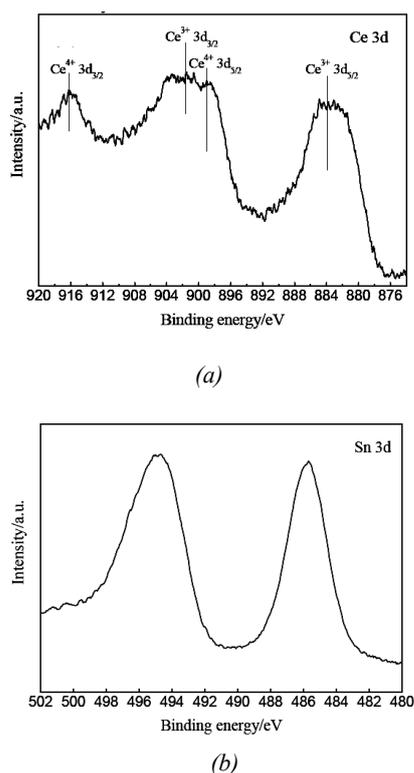
Fig. 3. XPS of Ce 3d for CT (a) and (b) Sn 3d for ST.

The survey spectrum for Ce 3d region of the CT is shown in Fig. 3*(a)*. It is well known that XPS Ce 3d spectral of cerium compounds are complicated due to hybridization of the Ce 4f with ligand orbitals and fractional occupancy of the valence 4f orbitals.[26] As shown, peaks located at 898.1 and 915.9 eV probably correspond to Ce^{4+} $3d_{5/2}$ and Ce^{4+} $3d_{3/2}$, and peaks located at 884.0 and 901.6 eV may belong to Ce^{3+} $3d_{5/2}$ and Ce^{3+} $3d_{3/2}$ [27]. Two different explanations about the source of the Ce^{3+} in CeO_2 have been suggested. B. M. Reddy and his coworkers have published a series of articles, which reported that Ce (III) existed in CeO_2-SiO_2 [28], CeO_2-TiO_2 [29] and CeO_2-ZrO_2 [30] catalysts by using XPS measurement, however, Ce_2O_3 can not be detected from XRD measurements, they proposed that the occurrence of partial photoreduction of CeO_2 during the XPS measurement is probably due to the progressive elimination of surface hydroxyls and oxygen ions from the CeO_2 surface upon vacuum treatment [28-30]. Whereas, Tsunekawa et al. insisted a different idea, which demonstrated that for CeO_2 nanocrystals with a particle size of several nanometers, Ce^{4+} ions near the surface will convert to Ce^{3+} ions and the fraction of Ce^{3+} ions increased with decreasing particle size [31-33]. Same results were also reported by Wang et al. [27] and Wu et al. [34], who supported Tsunekawa's propositions.

AFM was carried out to characterize the surface morphology of the film. Fig. 4 shows 2-D and 3-D AFM images of the surface of ST, CT and SCT deposited on ITO glass, respectively. As shown in Fig. 4a, the surface for ST is relatively uniform and the film is composed of the monodisperse spherical particles with average particle size about 48 nm. For the CT and SCT, the evaluated average particle size is about 11.5 and 5.9 nm, which is much smaller than that of ST. The mean square roughness of the ST, CT and SCT are 7.3, 2.3 and 1.4 nm, respectively.
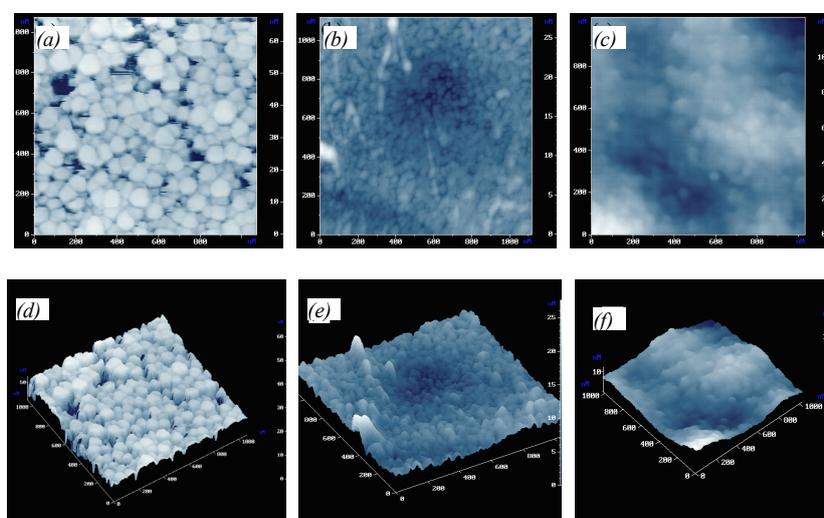
Fig. 4. 2-D images for (a)ST, (b) CT, (c) SCT and 3-D images for (d)ST, (e) CT and (f) SCT.

The UV-vis absorption spectra of the three doped films and the pure TiO_2 film over the wavelength rang of 200~600 nm is presented in Fig. 5. The presence of the absorbance peaks around 250nm and 300nm is due to the glass substrate. All the doped TiO_2 films exhibited wavy nature around the absorption edge region with respect to the pure TiO_2 film. It can been seen that the absorption edge of CT has a red shift compared with that of the pure TiO_2 film, while for the ST the red shift is not so evident as that of CT. In the ultraviolet region, the absorption intensities of the doped TiO_2 thin films are stronger than the pure TiO_2 film.
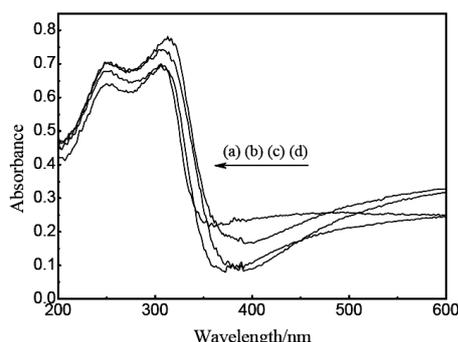
Fig. 5. UV-vis spectra of (a) pure film (b) ST, (c) SCT and (d) CT.

According to the data of the absorption spectra, the band gap (E_g) of the TiO_2 can be estimated by using the equation: $\alpha h v = A(hv - E_g)^n$, where $n=1/2$ for direct transmission and $n=2$ for indirect transmission, hv is the photon energy, α is the absorption coefficient [27]. Fig. 6 is given basing on the above equation. In order to estimate the band gaps of the TiO_2 films for the indirect transmission, the plots $(\alpha h v)^{1/2}$ versus hv are drawn for all the films and are shown in Fig.6 which is obtained by extrapolating the tangent to the plot to $(\alpha h v)^{1/2} = 0$. The evaluated E_g (3.28 eV) of pure TiO_2 is larger than the theoretic value of 3.2 eV and the band gap of the CT, SCT and ST are found to be 3.04, 3.13 and 3.26 eV, respectively. Clearly, the doping of Sn and Ce can narrow the band gap of TiO_2 and this effect of CT is stronger than that of other two kinds of films.
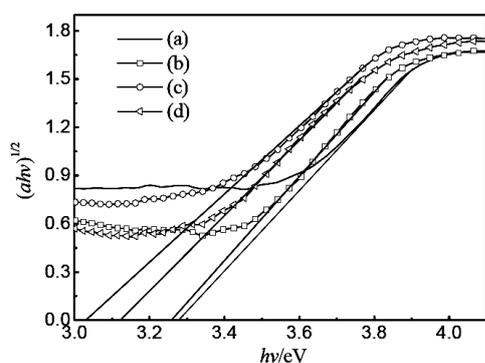
Fig. 6. Plots of $(\alpha h v)^{1/2}$ vs. hv for (a) pure film (b) ST, (c) CT and (d) SCT.

In conclusion, doping Sn and Ce caused the absorption edge of TiO_2 shifted towards visible light region and contributed to the band gap narrowing, indicating that doping can improve optical property of TiO_2 film in visible light region, which will probably make a good foundation for the investigation of TiO_2 films applied in photovoltaic fields.

4. Conclusions

ST, CT and SCT prepared through sol-gel dip coating process have been investigated. XRD patterns of powder samples showed only characteristic peaks of anatase TiO_2 but no crystalline phases of compounds formed by doping ions due to their small amount. According to the XPS results, Sn existed in the form of Sn^{+4} and Ce existed in two forms (Ce^{3+} and Ce^{4+}). AFM indicated that films are composed of the monodisperse spherical particles. In addition, UV-vis absorption spectra revealed that the absorption edge of TiO_2 shifts towards visible light region via doping Sn and Ce, indicating that doping may improve the photoresponse of TiO_2 film in visible light region.

References

[1] X. W. Zhang, M. H. Zhou, L. C. Lei, Catal. Commun. **7**, 427 (2006).
[2] S. M. Chiu, Z. S. Chen, K. Y. Yang, Y. L. Hsu, D. Gan, J. Mater. Process. Tech. **192-193**, 60 (2007).
[3] F. Edelman, H. Hahn, S. Seifried, C. Alof, H. Hoche, A. Balogh, P. Werner, K. Zakrzewska, M. Radecka, P. Pasierb, A. Chack, V. Mikhelashvili, Mater. Sci. Eng. **B 60-70**, 386 (2000).
[4] A. M. Ruiz, G. Sakai, A. Cornet, K. Shimanoe, J. R. Morante, N. Yamazoe, Sensor. Actuator B-Chem. **93** 509 (2003).
[5] P. Pichat, J. Disdier, C. Hoang-Van, D. Mas, G. Goutailler, C. Gaysse, Catal. Today **63**, 363 (2000).
[6] T. F. Xie, D. J. Wang, L. J. Zhu, T. Li, Y. J. Xu. Mater. Chem. Phys. **70**, 103 (2001).
[7] S. Lee, Y. Jun, K. J. Kim, D. Kim, Sol. Energy Mater Sol. Cells, **65**, 193 (2001).
[8] P. T. Hsiao, K. P. Wang, C. W. Cheng, H. Teng, J. Photoch. Photobio. A: Chem **188**, 19 (2007).
[9] K. E. Kim, S. R. Jang, J. Park, R. Vittal, K. J. Kim, Sol. Energy Mater. Sol. Cells **91**, 366 (2007).
[10] W. W. Zhang, Y. Q. Chen, S. Q. Yu, S. G. Chen, Y. S. Yin, Thin Solid Films **516**, 4690 (2008).

[11] X. B. Chen, S. S. Mao, Chem. Rev. **107**, 2891 (2007).

[12] C. Wang, T. M. Wang, S. K. Zheng, Physica E **14**, 242 (2002).

[13] S. Mahanty, S. Roy, S. Sen, J. Cryst. Growth **261**, 77 (2004).

[14] F. Gracia, J. P. Holgado, L. Contreras, T. Girardeau , A. R. González-Elipe, Thin Solid Films **429**, 84 (2003).

[15] Y. K. Du, Y. Q. Gan, P. Yang, F. Zhao, N. P. Hua, L. Jiang, Thin Solid Films **491**, 133 (2005).

[16] J. Domaradzki, Thin Solid Films **497**, 243 (2006).

[17] J. H. He, I. Ichinose, S. Fujikawa, Chem. Mater. **14**, 3493(2002).

[18] C. G. Wu, L. F. Tzeng, Y. T. Kuo, C. H. Shu., Appl. Catal. **A 226**, 199 (2002).

[19] T. Umeb**a**yashi, T. Yamaki, H. Itoh, K. Asai, Appl. Phys. Lett. **81**, 454 (2002).

[20] J. H. Pan, W. I. Lee, Chem. Mater.   **18**, 847 (2006).

[21] T. Lindgren, J. M. Mwabora, E. Avendano, J. Jonsson, A. Hoel, C. G. Granqvist, S. E. Lindquist, J. Phys. Chem. **B107**, 5709 (2003).

[22] G. R. Torres, T. Lindgren, J. Lu, C. G. Granqvist, S. E. Lindquist, J. Phys. Chem. **B108**, 5995 (2004).

[23] H. B. Jiang, L. Gao, Mater. Chem. Phys. **77**, 878 (2002).

[24] Y. K. Du, Y. Q. Gana, P. Yang, Z. Cuie, N. P. Hua, Mater. Chem. Phys. **103**, 446 (2007).

[25] T. Moon, S. T. Hwang, D. R. Jung, D. Son, C. Kim, J. Kim, M. Kang and, B. Park, J. Phys. Chem. **C111**, 4164 (2007).

[26] P. W. Park, J. S. Ledford. Effect of Crystallinity on the Photoreduction of Cerium Oxide, Langmuir **12**, 1794 (1996).

[27] A. L. Wang, Z. W. Quan, J. Lin, Inorg. Chem. **46**, 5237 (2007).

[28] B. M. Reddy, A. Khan, Y. Yamada, T. Kobayashi, S. Loridant, J. C. Volta, J. Phys. Chem. **B106**, 10964 (2002).

[29] B. M. Reddy, A. Khan, Y. Yamada, T. Kobayashi, S. Loridant, J. C. Volta, J. Phys. Chem. **B107**, 5162 (2003).

[30] B. M. Reddy, A. Khan, Y. Yamada, T. Kobayashi, S. Loridant, J. C. Volta, Langmuir **19**, 3025 (2003).

[31] S. Tsunekawa, T. Fukuda, A. Kasuya, Surf. Sci. **457**, L437 (2000).

[32] S. Tsunekawa, R. Sahara, Y. Kawazoe, K. Ishikawa Appl. Surf. Sci. **152**, 53 (1999).

[33] S. Tsunekawa, R. Sivamohan, S. Ito, A. Kasuya, T. Fukuda, Nanostruct. Mater. **11**, 141 (1999).

[34] L. J. Wu, H. J. Wiesmann, A. R. Moodenbaugh, R. F. Klie, Y. M. Zhu, D. O. Welch, M. Suenaga, Phys. Rev. **B69**, 125415:1-9 (2004).

[*]Corresponding author: hmyang9392@hotmail.com